

Maximum Power Point Determination of Bifacial PV Using Multi-Verse Optimization Algorithm Applied on Different Cell Models

xxxx

Angela Najdoska*, Goga Cvetkovski*

Faculty of Electrical Engineering and Information Technologies, Ss. Cyril and Methodius University, Department of Electrical Machines, Transformers and Apparatuses, Rudjer Boskovic 18, P. O. Box 574, 1000 Skopje, North Macedonia

Received: 24 December, 2024; Accepted: 24 February, 2025

Abstract: In the design process of a photovoltaic (PV) power plant, determination of the maximum power that can be extracted from the PV modules is essential, especially for the dimensioning of the individual parts of the plant. This paper presents the determination of the maximum power point (MPPT) of a bifacial PV system using three different cell models. The optimal power point is determined by using a novel multi-verse optimization (MVO) algorithm as the optimization tool. In this research work the MPPT of bifacial PV modules is determined by using the following three PV cell models: ideal single diode model, real single diode model, and two-diode model of PV cell. These cell models are developed for single-sided PV modules and therefore a proper modification of the models is necessary in order to be applied for the investigated modules. The purpose of this optimization procedure is to determine the maximum power of a bifacial PV module by minimizing the power difference between the calculated power and the experimentally determined power for certain atmospheric conditions.

Keywords: PV cell • bifacial module • multi-verse optimization algorithm • maximum power point • PV cell equivalent circuit

1. Introduction

The increasing demand for electricity has driven engineers to develop more efficient photovoltaic (PV) technologies, leading to the rise of bifacial PV cells. These cells can generate more electricity per unit area, prompting a surge in the construction of bifacial PV power plants in North Macedonia over the past 2 years. Some existing plants are even retrofitting their infrastructure by replacing monofacial modules with bifacial ones. Bifacial PV modules are highly efficient, absorbing light and generating power from both their front and rear surfaces. This dual-sided absorption results in greater power output per area compared with conventional monofacial modules (Berrian et al., 2019; Jang and Lee, 2020; Lames et al., 2018; Leonardi et al., 2021; Mesquita et al., 2019). While the front-side power generation, like that of monofacial modules, depends on weather conditions such as solar irradiation and temperature, the rear-side generation is further influenced by varying reflective conditions (Sun et al., 2018). Beyond increased power generation, bifacial PV panels offer significant environmental benefits. By harnessing solar energy on both sides, they require less land for installations, maximizing land use and preserving natural habitats. Furthermore, bifacial modules contribute to lower per-unit energy costs (per kW/h). Their greater efficiency translates to a lower levelized cost of electricity (LCOE), making them particularly attractive for large-scale deployments where maximizing output while minimizing cost is crucial. Bifacial solar panels can generate up to 20% more energy per panel per day compared with traditional panels. While the initial cost of bifacial modules

* Emails: anenajd9@gmail.com; gogacvet@feit.ukim.edu.mk

is higher than that of monofacial modules, the increased energy production and resulting cost savings over time lead to faster payback periods (Badran and Dhimish, 2024). In essence, the higher upfront investment is offset by long-term economic advantages.

Therefore, a reliable PV system model must consider several key parameters for any type of analysis, including solar irradiation, ambient temperature, and module bifaciality (Guerrero-Lemus et al., 2016), which is influenced by the reflective conditions of the ground. Implementing such a model in the design phase of a PV power plant is crucial for optimizing efficiency and selecting appropriate electrical equipment, particularly the inverter.

While advancements in solar cell and PV module efficiency are ongoing, a growing number of PV power generation systems are being installed without adequate consideration of the surrounding environment. This oversight can lead to significant power losses due to shading from nearby structures or vegetation, as well as varying weather and ground conditions. Shading, in particular, can cause solar cells to act as loads, consuming power and generating heat instead of producing electricity (Fatih et al., 2017; Fatih and Hakan, 2020; Torres et al., 2018). The determination of the maximum power point (MPPT) in such conditions can also be a challenge and therefore, a stochastic approach is needed (Bettahar et al., 2024). Different ground types can also affect the power output of a PV plant.

Therefore, accurately determining the maximum power output for a given location, considering both ground and weather conditions, is essential. This is particularly important in regions with above-average solar irradiation under certain atmospheric conditions. In such cases, a rapid and reliable method is needed to analyze numerous combinations of solar irradiation and temperature to generate sufficient data for proper plant dimensioning. Nature-inspired optimization methods are well-suited for this task due to their stochastic nature, multiple starting points, and ability to explore a wide range of solutions. Previous work by the authors has explored the application of genetic algorithms (GA) (Holland, 1995) and particle swarm optimization (Kennedy and Eberhart, 1995) to single-sided PV modules (Najdoska and Cvetkovski, 2022). While these methods yielded good results, this study investigates the performance of the novel multi-verse optimization (MVO) algorithm. A key advantage of MVO is its adaptive search parameters, unlike the fixed crossover and mutation probabilities used in GA. These variable parameters tend to improve the reliability and quality of the search and the resulting solution. This work implements the MVO algorithm to determine the MPPT and PV cell parameters. The PV cells are represented by a mathematical model derived from an appropriate equivalent circuit. Three types of equivalent circuits are investigated: the ideal single-diode model, the real single-diode model, and the two-diode model.

The following sections first present the MVO algorithm. Then, the mathematical models of the investigated PV cell equivalent circuits are elaborated upon. This is followed by a presentation of the optimization results for the different PV cell models under varying solar irradiation levels. Finally, the conclusions are drawn from the presented results.

2. MVO Algorithm

The following text briefly describes the MVO algorithm, a novel optimization concept inspired by cosmology and theoretical physics, specifically the Big Bang Theory.

The Big Bang Theory (Tegmark, 2004) proposes that the universe originated from a massive explosion, leading to the expansion and evolution of the cosmos. It suggests that everything we observe today originated from this initial event. In contrast to the single-universe concept, the Multi-Verse Theory (Eardley, 1974; Steinhardt and Turok, 2002) proposes the existence of multiple universes, each potentially with its own unique set of physical laws, properties, and histories. The simultaneous existence of multiple universes is a compelling area of speculation in cosmology. The MVO algorithm draws inspiration from concepts within the Multi-Verse Theory, namely, white holes, black holes, and wormholes (Mirjalili et al., 2015; Sayed, G. I., Darwish, A. and Hassanien, A. E. 2018). These are hypothetical constructs in theoretical physics with intriguing properties as below:

- *White holes*: Theoretical regions of space–time that expel matter and energy outward, contrasting with black holes which draw matter and energy inward (Davies, 1978). White holes are like the reverse of black holes.
- *Black holes*: Regions of space–time with gravitational pull so strong that nothing, not even light, can escape from them. They are formed from the collapse of massive stars.

- *Wormholes*: Hypothetical tunnels or shortcuts through space–time that could potentially connect distant points in the universe or even different universes (Morris and Thorne, 1988).

Within the context of optimization algorithms, these cosmological concepts are used metaphorically to guide the search process. White holes, for example, might represent the exploration of new solutions, while black holes could symbolize convergence toward promising solutions. Wormholes might represent paths connecting different regions of the search space. Conceptual models of white holes, black holes, and wormholes are used to visually represent how these concepts are integrated into the MVO algorithm (see Figure 1). These models likely aid in understanding the algorithm's function and how it mimics processes inspired by cosmological theories. This interdisciplinary approach to optimization, drawing inspiration from theoretical physics, is innovative and thought-provoking. It demonstrates how ideas from one scientific field can be creatively applied to solve problems in another, potentially leading to novel solutions and insights.

The following text provides a brief introduction to the MVO algorithm. A more detailed explanation of the algorithm's performance, mathematical background, and comparison with other optimization methods can be found in the original paper by its authors (Mirjalili et al., 2015). The MVO optimization process begins by creating a set of random universes. In this algorithm, each solution represents a universe, and each variable within the solution represents an object in that universe. During each iteration, objects in universes with high expansion rates tend to move toward universes with low expansion rates via white/black holes. Simultaneously, every universe experiences random teleportation of its objects through wormholes toward the best universe found so far. This process continues until a stopping criterion is met, which in this case is the maximum number of iterations. The computational complexity of the algorithm depends on the number of iterations, the number of universes, the roulette wheel mechanism, and the universe sorting mechanism. The quality of the search is ensured by two key mechanisms: exploration and exploitation. Exploration helps the algorithm cover a broad search area and identify potentially good solutions (universes). Exploitation, conversely, improves convergence around promising solutions identified during the exploration phase. A proper balance between these two mechanisms ensures convergence toward the global optimum (Arunachalam, 2022).

The algorithm also incorporates two main coefficients that fine-tune the search: the wormhole existence probability (WEP) and the traveling distance rate (TDR). The WEP coefficient defines the probability of wormhole existence in universes. It is typically increased linearly over the iterations to emphasize exploitation as the optimization process progresses. TDR defines the distance rate (variation) that an object can be teleported by a wormhole around the best universe found so far. The TDR is also increased over the iterations to enable a more precise exploitation/local search around this best-obtained universe. The variability of these coefficients tends to improve the reliability and quality of the search.

In Figure 2 the block diagram of the MVO algorithm is presented. Some aspects of the algorithm in context of the multi-universe theory are presented below.

The following observations highlight the algorithm's potential for solving optimization problems:

- Universes with high inflation (expansion) rates are more likely to generate white holes, enabling them to send objects to other universes and improve their inflation rates.



(a) White hole

(b) Black hole

(c) Wormhole

Figure 1. Conceptual models of white hole, black hole and wormhole components.

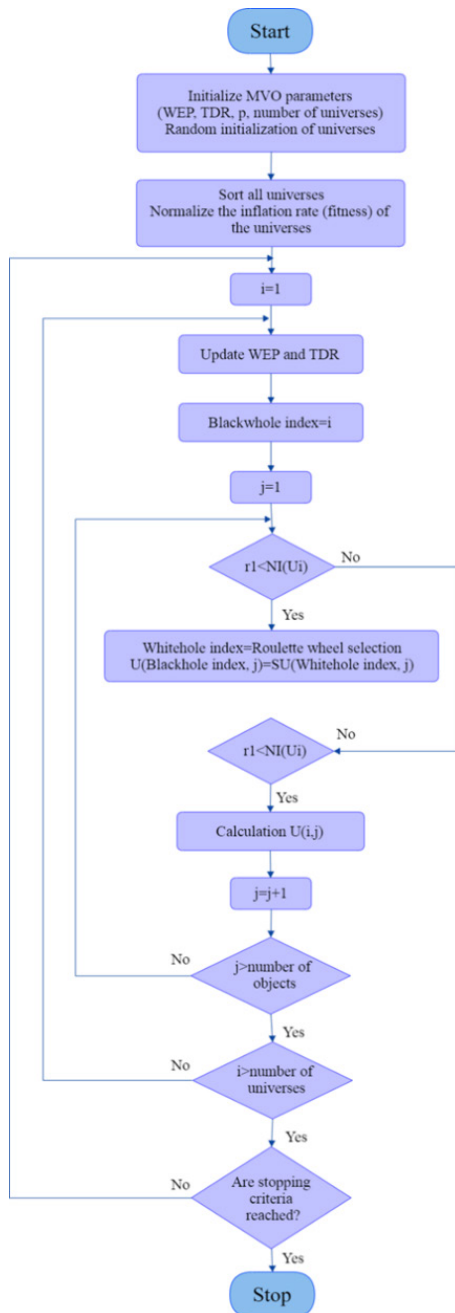


Figure 2. MVO algorithm presentation. MVO, multi-verse optimization; TDR, traveling distance rate; WEP, wormhole existence probability.

- Universes with low inflation rates are more likely to contain black holes, increasing their probability of receiving objects from other universes. This mechanism contributes to improving the overall expansion rates of universes.
- Wormholes tend to appear randomly in any universe, regardless of inflation rate, helping maintain diversity across universes throughout the iterations.
- White/black hole tunnels require universes to undergo abrupt changes, which promotes exploration of the search space and helps resolve local optima stagnation. Wormholes randomly redistribute some variables of universes around the best solution found so far, ensuring exploitation around the most promising region of the search space.

- Adaptively increasing WEP values smoothly increases the probability of wormholes appearing in universes, emphasizing exploitation during the optimization process. Adaptively decreasing TDR values reduce the travel distance of variables around the best universe, improving the accuracy of local search over iterations.

The convergence of the proposed algorithm is ensured by introducing exploitation/local search proportional to the number of iterations. In this investigation, the number of universes is set to 50, and the number of iterations to 200.

3. Bifacial PV Modules

This section provides a brief introduction to the parameters and characteristics of the analyzed bifacial module. The module investigated is a bifacial monocrystalline p-type module manufactured using PERC technology. Table 1 shows the characteristics of the tested bifacial module under standard test conditions (STC) (Irradiance 1,000 W/m², Cell Temperature 25°C, Air Mass AM1.5). The data presented in Tables 1 and 2 for the investigated module are taken from: (<https://www.jasolar.com/uploadfile/2022/0511/20220511055529246.pdf>).

Table 2 shows the characteristics of the module, if bifaciality of 10% is implemented. This value is also used in the optimization procedure to define the solar irradiation on the rear side of the PV module.

4. Equivalent Circuit PV Models

For the numerical analysis and MPPT determination of both monofacial and bifacial PV modules, an appropriate and accurate equivalent circuit model is crucial. Numerous models for monofacial modules exist in the literature. This research focuses on three of these: the simplest, the ideal single-diode PV cell model (Bellini et al., 2009), which has four unknown parameters; the more realistic real single-diode PV cell model (Ishaque et al., 2011a,b), with six unknown parameters; and the two-diode PV cell model (Ishaque et al., 2011a,b), which has seven unknown parameters. While the three-diode PV cell model (Qais et al., 2022) is also documented, it will not be explored in this work, but will be considered in future research.

Table 1. Standard parameters of the analyzed module given by the producer

Parameters	Unit	Values
Peak power	(Wp)	540
Maximum voltage per MPPT	(V)	41.64
Maximum current per MPPT	(A)	12.97
Open circuit voltage	(V)	49.60
Short circuit current	(A)	13.86
Efficiency	(%)	20.9
Area of the module	(m ²)	2.58

Table 2. Parameters of the analyzed module given by the producer with included bifaciality of 10%

Parameters	Unit	Values
Peak power	(Wp)	578
Maximum voltage per MPPT	(V)	41.65
Maximum current per MPPT	(A)	13.88
Open circuit voltage	(V)	49.93
Short circuit current	(A)	14.93
N_s	(# of cells)	60
K_I	(%/°C)	0.00543
K_V	(%/°C)	-0.136
G_{STC}	(W/m ²)	1,000

STC, standard test conditions.

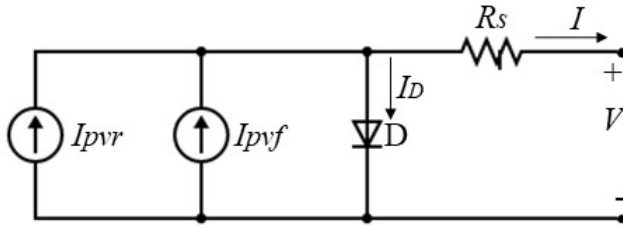


Figure 3. Ideal single diode PV cell model. PV, photovoltaic.

All three models will be adapted to account for the bifacial nature of the modules under investigation.

4.1. Ideal single-diode PV cell model

The ideal solar cell circuit consists of a single diode (D) connected in parallel with light-generated current sources for the front (I_{pvf}) and rear (I_{pvr}) sides of the cell, and a series resistance R_s , as shown in Figure 3. This series resistance arises from the bulk resistance of the semiconductor material, the bulk resistance of the metal electrodes, and the contact resistance between the semiconductor and metal. Careful design of the top contact and emitter resistance can control the series resistance (Sukhatme, 1984). A low series resistance is crucial for optimal solar cell efficiency, as a higher value reduces the short-circuit current (Dhankhar et al., 2014). The output current I from in Figure 3 can be determined as: $I = I_{pvf} + I_{pvr} - I_D$.

While in a more detailed form it can be expressed as:

$$I = I_{pvf} + I_{pvr} - I_D \left[\exp \left(\frac{V_{mp} + I_{mp} R_s}{a V_T} \right) - 1 \right] \quad (1)$$

where: I_{pvf} and I_{pvr} are the cell light generated currents at the front and rear sides of the PV cell, respectively; I_D is the reverse saturation current of the diode D and it is defined by the material properties of the PV cell; $V_T = (N_s / kT) / q$ is the thermal voltage of the PV module having N_s cells connected in series; q is the electron charge ($1.60217646/10^{-19}$ C); k is the Boltzmann constant ($1.3806503/10^{-23}$ K); T is the temperature of the p-n junction in Kelvins and a is the diode ideality factor and in this investigation is taken to be equal to 1. In Eq. (1), the front and rear cell light generated current can be determined using the following equations given by Bhang et al. (2019) and Ishaque et al. (2011a,b):

$$I_{pvf} = (I_{pv_{stc}} + K_f \Delta T) \frac{G_f}{G_{stc}} \quad (2)$$

$$I_{pvr} = (I_{pv_{stc}} + K_r \Delta T) \frac{G_r}{G_{stc}} \quad (3)$$

where: $I_{pv_{stc}}$ is the light generated current at STC, $\Delta T = T - T_{stc}$ ($T_{stc} = 25^\circ\text{C}$); G_f and G_r are the surface irradiance of the cell on the front and on the rear side, respectively and G_{stc} is the irradiance at STC. K_f is the short-circuit current coefficient, normally provided by the manufacturer. In this investigation the rear side irradiance is taken to be 10% of the front irradiance, whatever it is, for a certain optimization process. In Eq. (1), the reverse saturation current of the diode D can be determined using the following equation defined in Ishaque et al. (2011a,b):

$$I_D = \frac{(I_{sc_{stc}} + K_i \Delta T)}{\exp \left[\left(\frac{V_{oc_{stc}} + K_v \Delta T}{a V_T} \right) \right] - 1} \quad (4)$$

The constant K_v is the open circuit voltage coefficient and it is available from the datasheet given by the producer. The same applies for the short-circuit current at STC $I_{sc_{stc}}$. The last parameter in Eq. (1) that has not been defined is the series resistance R_s . This series resistance in a solar cell comprises three parts: the first part is defined by

the movement of current through the emitter and base of the solar cell; the second part is the contact resistance between the metal contact and silicon; and finally the resistance of the top and rear metal contacts. Till date, in the literature are a large number of papers dealing with the determination of the cell parameters including R_s and the calculation approaches can be divided into three groups: analytical (Bissels et al., 2014; Ndegwa et al., 2020), numerical iterative procedure (Ćalasan et al., 2021; Xiao et al., 2004), and experimental approach in which the cell resistances are determined based on the measured I–V characteristics of the investigated PV cells (Hansen and King, 2019). This work introduces a novel approach for determining the series resistance (R_s). Initially, a simplified method (Bellini et al., 2009) is used to estimate R_s . Subsequently, during the optimization process, this initial value is allowed to vary within the defined upper and lower limits for fine-tuning. This two-step approach is adopted because the series resistance is partially dependent on solar irradiation intensity (Villalva et al., 2009). This method avoids complex and time-consuming calculations. The following text presents the equations used to determine the initial R_s value, derived from the ideal single-diode PV cell model. Based on this approach (Fahim et al., 2022), the output voltage of a PV module is defined as follows:

$$V = C_2 \cdot V_{oc} \cdot \ln \left[1 + \left(\frac{\left(1 - \frac{I_{mp}}{I_{sc}} \right)}{C_2} \right) \right] \quad (5)$$

where

$$C_1 = \left(1 - \frac{I_{mp}}{I_{sc}} \right) \exp \cdot \left(\frac{-V_{mp}}{C_2 V_{oc}} \right) \quad (6)$$

$$C_2 = \frac{\left(\frac{V_{mp}}{V_{oc}} - 1 \right)}{\ln \left(1 - \frac{I_{mp}}{I_{sc}} \right)} \quad (7)$$

The value of the series resistance R_s can be calculated by deriving Eq. (5) with the current calculated for $I = 0$ as follows:

$$R_s = \left(C_2 \cdot \frac{V_{oc}}{I_{sc}} \right) \cdot \left(\frac{1}{1 + C_1} \right) \quad (8)$$

Based on these equations the calculated value of the series resistance for the investigated bifacial module R_s is 0.2033 ohms.

4.2. Real single-diode PV cell model

The real solar cell circuit presentation consists of a single diode (D) connected in parallel with light generated current sources for the front (I_{pvr}) and rear (I_{pvf}) sides of the cell, a parallel connected resistance R_p and in series connected resistance R_s , as shown in Figure 4. The shunt resistance (R_p) is caused by leakage across the p-n junction, impurities, and crystal defects. Ideally, the shunt resistance should be high; a low value reduces the open-circuit

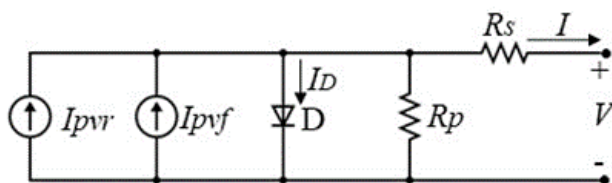


Figure 4. Real single-diode PV cell model. PV, photovoltaic.

voltage. Both series and shunt resistance losses decrease the efficiency and fill factor of the solar cell (Dhankhar et al., 2014). The output current I can be determined based on the presented circuit in Figure 4, as follows:

$$I = I_{pvf} + I_{pvr} - I_D \left[\exp \left(\frac{V_{mp} + I_{mp} R_s}{a V_{T1}} \right) - 1 \right] - \left(\frac{V_{mp} + I_{mp} R_s}{R_p} \right) \quad (9)$$

where all the parameters are presented previously. Additionally, in this model the parallel connected resistance R_p can be determined using Eq. (10):

$$R_p = \frac{V_{mp} + I_{mp} \cdot R_s}{\left\{ (I_{pvf} + I_{pvr}) - I_D \left[\exp \left(\frac{(V_{mp} + I_{mp} \cdot R_s)}{V_T} \right) + \exp \left(\frac{(V_{mp} + I_{mp} \cdot R_s)}{(p-1)V_T} \right) + 2 \right] - \frac{P_{max,E}}{V_{mp}} \right\}} \quad (10)$$

4.3. Two-diode PV cell model

The two-diode electrical model of a solar PV cell is generally considered more accurate than the single-diode model because it accounts for the effects of recombination. This PV cell model more accurately reflects the impact of changing weather conditions (Alrahim Shannan et al., 2013) compared with the single-diode model. The two-diode model (Ishaque et al., 2011a,b) is shown in Figure 5.

Using this model, greater accuracy can be achieved in comparison with the one-diode model, although in the case of the two-diode model it requires a computation of eight parameters: I_{pvf} , I_{pvr} , I_{D1} , I_{D2} , R_p , R_s , a_1 and a_2 . The PV current can be described as a function of temperature and irradiance:

$$I = I_{pvf} + I_{pvr} - I_{D1} \left[\exp \left(\frac{V_{mp} + I_{mp} R_s}{a_1 V_{T1}} \right) - 1 \right] - I_{D2} \left[\exp \left(\frac{V_{mp} + I_{mp} R_s}{a_2 V_{T2}} \right) - 1 \right] - \left(\frac{V_{mp} + I_{mp} R_s}{R_p} \right) \quad (11)$$

All the parameters in Eq. (11) are previously explained in the single-diode model, while the coefficients a_1 and a_2 are the ideality factors of the first and second diodes, consequently. In accordance with Shockley's diffusion theory, the diffusion current, a_1 must be unity. The value of a_2 , however, is flexible. Based on extensive simulation carried out (Ishaque et al., 2011a,b), it is found that if $a_2 \geq 1.2$, the best match between the proposed model and the practical I–V curve is observed. Since $(a_1 + a_2)/p = 1$ and $a_1 = 1$, it follows that the variable p can be $p \geq 2.2$. To maintain the same form as in Eq. (4), both the reverse saturation currents I_{D1} and I_{D2} are set to be equal in magnitude and can be determined using the following equation:

$$I_{D1} = I_{D2} = I_D = \frac{(I_{sc,STC} + K_I \Delta T)}{\exp \left[\left(\frac{V_{oc,STC} + K_V \Delta T}{\frac{(a_1 + a_2)}{p} V_T} \right) \right] - 1} \quad (12)$$

Therefore, Eq. (11) can be simplified and defined as follows:

$$I = I_{pvr} - I_D \left[\exp \left(\frac{V_{mp} + I_{mp} R_s}{V_T} \right) + \exp \left(\frac{V_{mp} + I_{mp} R_s}{(p-1)V_T} \right) + 2 \right] - \left(\frac{V_{mp} + I_{mp} R_s}{R_p} \right) \quad (13)$$

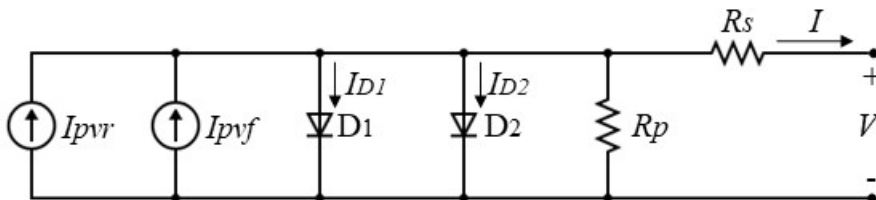


Figure 5. Two diode PV cell model. PV, photovoltaic.

The mathematical models of the investigated PV cell configurations are then implemented within the MVO algorithm, generating a set of results. These results are presented in the following section.

5. MVO Optimization Results

The purpose of this investigation is to determine the MPPT for a given location under various weather conditions. Therefore, the optimization process requires defining both the objective function and the optimization parameters. In this study, the objective function is defined as the difference between the maximum power calculated using the MVO algorithm ($P_{mppt,MVO}$) and the experimentally determined maximum power ($P_{mppt,catalog}$) provided by the manufacturer for specific weather conditions:

$$\text{Objective function} = \Delta P = P_{mppt,MVO} - P_{mppt,catalog} \quad (14)$$

The maximum output power of the PV module, as determined by the MVO algorithm, can be calculated using the following equation:

$$P_{mppt,MVO} = V_{mpp} \cdot I_{mpp} \quad (15)$$

The maximum power from the catalog data is determined similarly.

Since the MVO algorithm is a minimization algorithm, the optimization process aims to minimize the difference between the two power values as much as possible. The next step is to define the variable parameters that will be adjusted during optimization. Because the output current is calculated, the output voltage at maximum power conditions is defined as a variable. As mentioned in the descriptions of the single and two-diode models, the series resistance (R_s) is also a variable parameter. Each variable parameter is varied between user-defined lower and upper bounds, the values of which are presented in Table 3.

This research involved a series of MVO searches. Initially, an investigation was conducted to determine the optimal MVO algorithm parameters, specifically the number of iterations and universes. The optimization was performed with varying numbers of universes (from 10 to 100) and iterations (from 100 to 500). Based on the convergence rate of the objective function value and the computation time, the final parameter combination was set to 50 universes and 200 iterations. These values were chosen to balance accuracy and efficiency. The calculations were performed on a PC with an Intel(R) Core (TM) i5-6200U CPU @ 2.30 GHz processor and 8.00 GB of RAM. The computation time ranged from 10 s to 20 s, depending on the PV cell model, reflecting the linear nature of the problem. Subsequently, extensive optimizations were performed for the different PV cell models under varying solar irradiation levels at a constant temperature. The following text presents the objective function values and the optimized parameter values obtained from the best MVO search for each PV cell model at different solar irradiation levels.

5.1. Ideal single-diode PV cell model

The optimization results for the ideal single-diode PV cell model at irradiation of 1,000 W/m² are presented in Table 4, while the comparative optimization results for all the analyzed solar radiations are presented in Table 5.

The objective function value change during the iterations of the MVO search for a solar radiation of 1,000 W/m² is presented in Figure 6.

5.2. Real single-diode PV cell model

Table 6 presents the optimization results for the real single-diode PV cell model at an irradiation of 1,000 W/m², while Table 7 shows the comparative optimization results for all analyzed solar radiation levels.

Table 3. Optimization parameters and their optimization bounds

Variables	Description	Lower boundary	Upper boundary
V_{mppt} (V)	Voltage at MPPT	40	42
R_s (Ω)	PV cell series resistance	0.1	0.3

MPPT, maximum power point; PV, photovoltaic.

Table 4. Optimization data at 1,000 W/m²

Variables	Unit	Catalog data	MVO solution
V_{mppt}	(V)	41.65	41.6500004
R_s	(Ω)	/	0.20000967
ΔP	(W)	/	$5.373/10^{-6}$
P_{mppt}	(W)	578.102	578.102005

MVO, multi-verse optimization.

Table 5. Optimization data for other solar irradianctions

Parameter	Unit	Values		
		200(W/m ²)	600 (W/m ²)	1,000 (W/m ²)
V_{mppt}	(V)	40.160006	41.300002	41.6500004
R_s	(Ω)	0.1999898	0.201	0.20000967
ΔP	(W)	$3.215/10^{-5}$	$2.221/10^{-5}$	$5.373/10^{-6}$
$P_{mppt, MVO}$	(W)	110.44003	313.46702	578.102005
$P_{mppt, catalog}$	(W)	110.44	313.467	578.102005

MVO, multi-verse optimization.

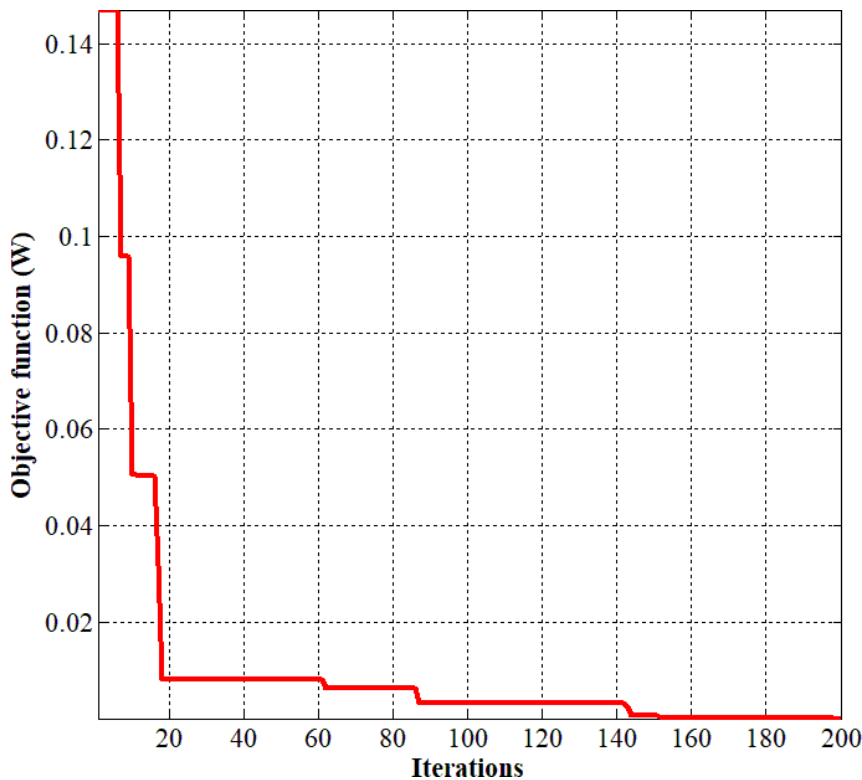


Figure 6. Objective function change during the MVO search for ideal single-diode model at 1,000 W/m². MVO, multi-verse optimization.

Figure 7 shows the change in the objective function value during the iterations of the MVO search at a solar radiation of 1,000 W/m² for the real single-diode PV cell model.

5.3. Two-diode PV cell model

Table 8 presents the optimization results for the two-diode PV cell model at an irradiation of 1,000 W/m², while Table 9 presents the comparative optimization results for all analyzed solar radiation levels.

Table 6. Optimization data at 1,000 W/m²

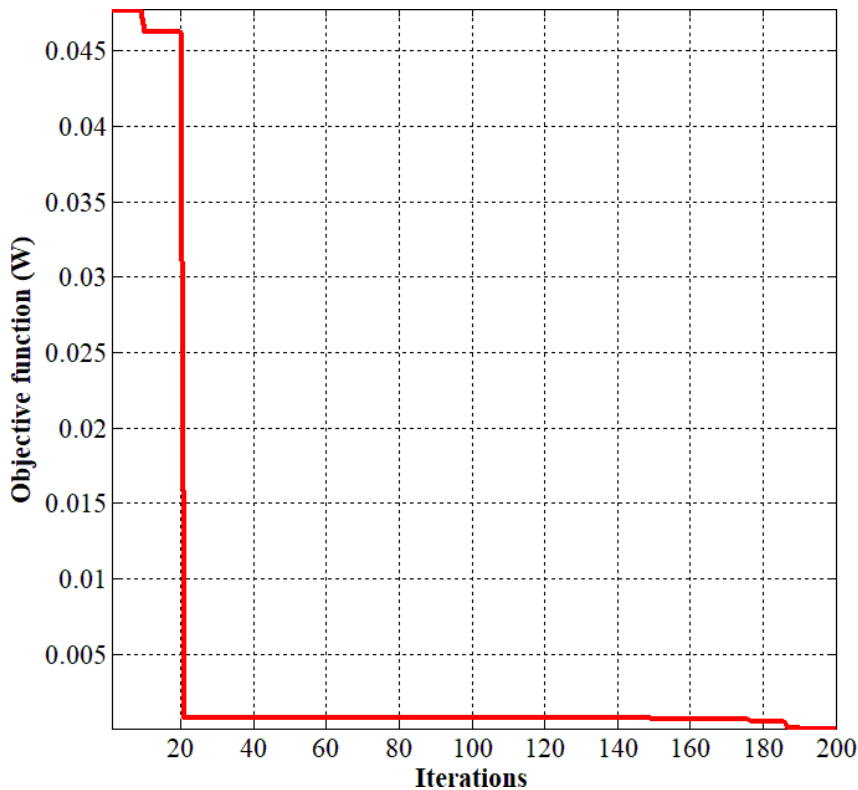
Variables	Unit	Catalog data	MVO solution
V_{mppt}	(V)	41.65	41.6500062
R_s	(Ω)	/	0.2
ΔP	(W)	/	$7.7617/10^{-5}$
P_{mppt}	(W)	578.102	578.102077

MVO, multi-verse optimization.

Table 7. Optimization data for other solar irradiances

Parameter	Unit	Values		
		200 (W/m ²)	600 (W/m ²)	1,000 (W/m ²)
V_{mppt}	(V)	40.1600006	41.3000048	41.6500062
R_s	(Ω)	0.19968144	0.20029	0.2
ΔP	(W)	$3.0929/10^{-6}$	$4.8763/10^{-6}$	$7.7617/10^{-5}$
$P_{mppt, MVO}$	(W)	110.4400031	313.4670049	578.102077
$P_{mppt, catalog}$	(W)	110.44	313.467	578.102077

MVO, multi-verse optimization.

**Figure 7.** Objective function change during the MVO search for real single-diode model at 1,000 W/m². MVO, multi-verse optimization.

The objective function value change during the iterations of the MVO search is presented in Figure 8.

The presented results demonstrate that the objective function achieves very small values, indicating that the calculated maximum power closely matches the experimentally determined maximum power provided by the manufacturer for the given meteorological conditions. These results suggest that the MVO algorithm is well-suited for determining the MPPT for the analyzed bifacial PV module, as well as other PV modules in general. The high quality of the results across the wide range of optimizations is attributable to the MVO algorithm's performance

Table 8. Optimization data at 1,000 W/m²

Variables	Unit	Catalog data	MVO solution
V_{mppt}	(V)	41.65	41.6500012
R_s	(Ω)	/	0.20019324
ΔP	(W)	/	$1.512/10^{-5}$
P_{mppt}	(W)	578.102	578.10202

MVO, multi-verse optimization.

Table 9. Optimization data for other solar irradiations

Parameter	Unit	Values		
		200 (W/m ²)	600 (W/m ²)	1,000 (W/m ²)
V_{mppt}	(V)	40.16001	41.3000064	41.6500012
R_s	(Ω)	0.2	0.2	0.20019324
ΔP	(W)	$4.872/10^{-5}$	$6.502/10^{-5}$	$1.512/10^{-5}$
$P_{mppt, MVO}$	(W)	110.44005	313.46707	578.10202
$P_{mppt, catalog}$	(W)	110.44	313.467	578.10202

MVO, multi-verse optimization.

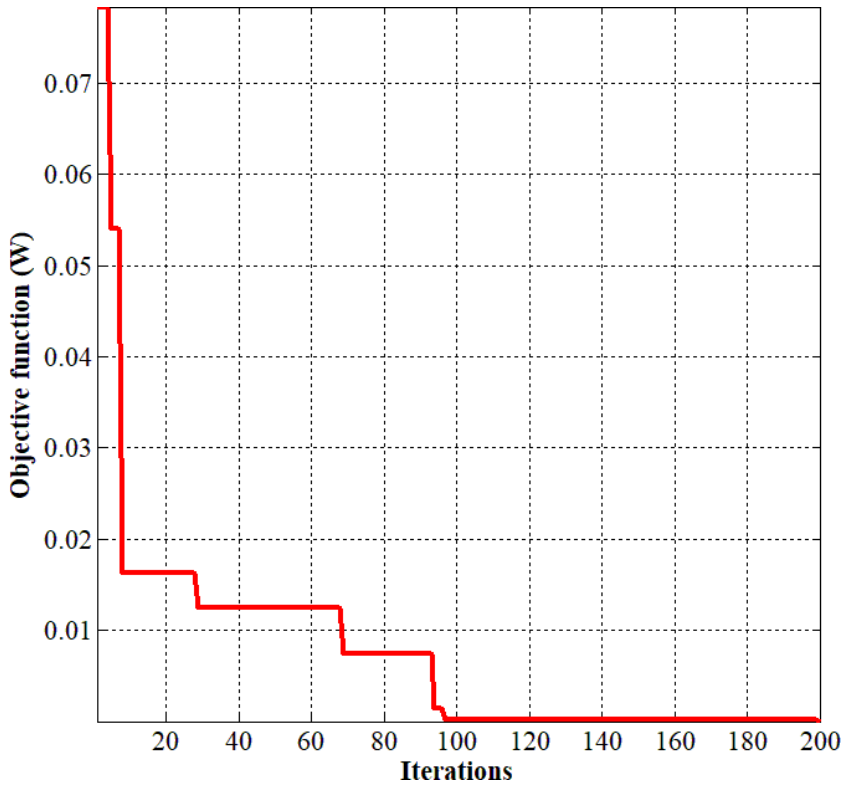


Figure 8. Objective function change during the MVO search for two-diode model at 1,000 W/m². MVO, multi-verse optimization.

parameters, namely, exploration and exploitation. These two parameters ensure a reliable and high-quality solution. Analysis of all results for the different PV cell models and solar irradiation levels shows that the algorithm consistently converges to a similar optimal solution, with differences in objective function values appearing only in the fifth or sixth decimal place. Regarding the implemented PV cell models, all three provided good results. Based on the objective function values, the real single-diode model performed slightly better than the other two, although

Table 10. Comparative optimization data at 1,000 W/m² and 20°C

Methods	Parameters		
	V_{mpp} (V)	P_{mpp} (W)	ΔP (W)
Catalogue data	41.65	578.102	/
MVO	41.6500004	578.10205	5.373/10 ⁻⁶
GA	41.362	578.11667	0.014674

GA, genetic algorithms; MVO, multi-verse optimization.

the two-diode model is theoretically more realistic. However, the two-diode model has more parameters that must be determined during optimization, and several coefficients that require tuning to improve its accuracy. Therefore, future work will focus on determining these coefficient values to enhance the two-diode model's accuracy. The slightly better performance of the real single-diode model compared with the ideal single-diode model is expected, as the real model is theoretically more accurate.

To validate the MVO optimization results, a comparison with another stochastic method is presented. In a previous study (Najdoska and Cvetkovski, 2024), the authors investigated the application of a GA (Holland, 1995) for determining the MPPT of an ideal single-diode bifacial PV cell model. Table 10 presents a comparison of the GA and MVO solutions for this model at 1,000 W/m² and 20°C. The data suggest that the MVO algorithm is more accurate in determining the MPPT compared with the catalog data than the GA. MVO also demonstrates greater computational efficiency, achieving a better solution with fewer iterations than GA. The robustness of the two methods is comparable.

Future work will involve similar optimization approaches using other algorithms, such as the teaching–learning-based optimization (TLBO) and the gravitational search algorithm (GSA). The plan is also to establish a test bed for the investigated PV panels to experimentally determine their I–V characteristics and cell parameters, comparing these experimental values with the optimized results. In the future investigations, different ground surfaces will be analyzed. Finally, the three-diode model will be implemented in the optimization process, and the results will be compared with those obtained from the other models investigated in this work.

6. Conclusion

In this research work an implementation of a physics-based optimization algorithm named MVO algorithm to determine the MPPT of a bifacial PV module is realized. Based on the presented results it can be concluded that the MVO algorithm is quite appropriate for determining the MPPT of a bifacial PV module for different weather conditions. The algorithm gives reliable and good optimization results. The determination of the MPPT using MVO algorithm was applied on three different PV cell models: ideal single-diode model, real single-diode model, and two-diode model. All the used models gave quite good optimization results and it can be concluded that for this application using the proposed algorithm, all of them can give useful results.

References

- Abrahim Shannan, N. M. A., Yahaya, N. Z. and Singh, B. (2013). Single-diode model and two-diode model of PV modules: A comparison. In *2013 IEEE International Conference on Control System, Computing and Engineering*, Penang, Malaysia, pp. 210–214.
- Arunachalam, S. (2022). Multi-Objective Multi Verse Optimization Algorithm to Solve Dynamic Economic Emission Dispatch Problem with Transmission Loss Prediction by an Artificial Neural Network. *Applied Soft Computing*, 124, p. 109021. doi: 10.1016/j.asoc.2022.109021
- Badran, G. and Dhimish, M. (2024). A Comparative Study of Bifacial Versus Monofacial PV Systems at the UK's Largest Solar Plant. *Clean Energy*, 8(4), pp. 248–260. doi: 10.1093/ce/zkae043
- Bellini, A., Bifaretti, S., Iacovone, V. and Cornaro, C. (2009). Simplified Model of a Photovoltaic

- Module. *Applied Electronics, Pilsen, Czech Republic*, pp. 47–51. <https://ieeexplore.ieee.org/document/5289294>
- Berrian, D., Libal, J. and Kelenk, M. (2019). Performance of Bifacial PV Arrays with Fixed Tilt and Horizontal Single-Axis Tracking: Comparison of Simulated and Measured Data. *IEEE Journal of Photovoltaics*, 9, pp. 1583–1589. doi: 10.1109/JPHOTOV.2019.2924394
- Bettahar, F., Sabrina, A., Achour, B. and Omar, C. (2024). A Comparative Study of PSO, GWO, and HOA Algorithms for Maximum Power Point Tracking in Partially Shaded Photovoltaic Systems. *Power Electronics and Drives*, 9(44), pp. 86–105. doi: 10.2478/pead-2024-0006
- Bhang, B. G., Lee, W., Kim, G. G., Choi, J. H., Park, S. Y. and Ahn, H.-K. (2019). Power Performance of Bifacial c-Si PV Modules with Different Shading Ratios. *IEEE Journal of Photovoltaics*, 9(5), pp. 1413–1420. doi: 10.1109/JPHOTOV.2019.2928461
- Bissels, G. M. M. W., Schermer, J. J., Asselbergs, M. A. H. and Haverkamp, E. J. (2014). Theoretical Review of Series Resistance Determination Methods for Solar Cells. *Solar Energy Materials and Solar Cells*, 130, pp. 605–614. doi: 10.1016/j.solmat.2014.08.003
- Ćalasan, M., Aleem, S. H. E. A. and Zobaa, A. F. (2021). A New Approach for Parameters Estimation of Double and Triple Diode Models of Photovoltaic Cells based on Iterative Lambert W Function. *Solar Energy*, 218, pp. 392–412. doi: 10.1016/j.solener.2021.02.038
- Davies, P. C. (1978). Thermodynamics of Black Holes. *Reports on Progress in Physics*, 41, pp. 1313–1355. doi: 10.1088/0034-4885/41/8/004
- Dhankhar, M., Singh, O. P. and Singh, V. N. (2014). Physical Principles of Losses in thin Film Solar Cells and Efficiency Enhancement Methods. *Renewable and Sustainable Energy Reviews*, 40, pp. 214–223. doi: 10.1016/j.rser.2014.07.163
- Eardley, D. M. (1974). Death of White Holes in the Early Universe. *Physical Review Letters*, 33(7), pp. 442–444. doi: 10.1103/PhysRevLett.33.442
- Fahim, S. R., Hasanien, H. M., Turkey, R. A., Abdel, A. H. E. and Calasen, M. (2022). A Comprehensive Review of Photovoltaic Modules Models and Algorithms Used in Parameter Extraction. *Energies*, 15(23), 8941, pp. 1–56. doi: 10.3390/en15238941
- Fatih, B., Gamze, E. and Hakan, F. O. (2017). Effects of Partial Shading on Energy and Exergy Efficiencies for Photovoltaic Panels. *Journal of Cleaner Production*, 164, pp. 58–69. doi: 10.1016/j.jclepro.2017.06.108
- Fatih, B. and Hakan, F. O. (2020). Effects of static and dynamic shading on Thermodynamic and Electrical Performance for Photovoltaic Panels. *Applied Thermal Engineering*, 169, pp. 1–25.
- Guerrero-Lemus, R., Vega, R., Kim, T., Kimm, A. and Shephard, L. E. (2016). Bifacial Solar Photovoltaics – A Technology Review. *Renewable and Sustainable Energy Reviews*, 60, pp. 1533–1549. doi: 10.1016/j.rser.2016.03.041
- Hansen, C. W. and King, B. H. (2019). Determining Series Resistance for Equivalent Circuit Models of a PV Module. *IEEE Journal of Photovoltaics*, 9(2), pp. 538–543. doi: 10.1109/JPHOTOV.2018.2883703
- Holland, J. H. (1995). *Adaptation in Natural and Artificial Systems*. Ann Arbor: University of Michigan Press.
- Ishaque, K., Salam, Z. and Taheri, H. (2011a). Simple, Fast and Accurate Two-Diode Model for Photovoltaic Modules. *Solar Energy Materials & Solar Cells*, 95(2), pp. 586–594. doi: 10.1016/j.solmat.2010.09.023
- Ishaque, K., Salam, Z. and Taheri, H. (2011b). Modelling and Simulation of Photovoltaic (PV) System During Partial Shading Based on a Two-Diode Model. *Simulation Modelling Practice and Theory*, 19, pp. 1613–1626. doi: 10.1016/j.simpat.2011.04.005
- Jang, J. and Lee, K. (2020). Practical Performance Analysis of a Bifacial PV Module and System. *Energies*, 13, pp. 1–13. doi: 10.3390/en13174389
- Jasolar.(2023) . Available at: <https://www.jasolar.com/uploadfile/2022/0511/20220511055529246.pdf>, Accessed date 20. September 2023.
- Kennedy, J. and Eberhart, R. (1995). Particle Swarm Optimization. *Proceedings of IEEE International Conference on Neural Networks*, vol.4, pp. 1942–1948. doi: 10.1109/ICNN.1995.488968
- Lames, M., Ozkalay, E., Gali, R. and Janssen, G. (2018). Temperature Effects of Bifacial Modules: Hotter or Cooler? *Solar Energy Materials and Solar Cells*, 185, pp. 192–197. doi: 10.1016/j.solmat.2018.05.033
- Leonardi, M., Corso, R., Milazzo, R. and Connelli, C. (2021). The Effects of Module Temperature on the Energy Yield of Bifacial Photovoltaics: Data and Model. *Energies*, 15, pp. 1–13. doi: 10.3390/en15010022
- Mesquita, D. D. B., Silva, J. L. D. S. and Moreira, H. S. (2019). A review and analysis of technologies

- applied in pv modules. In: *Proceedings of the 2019 IEEE PES Innovative Smart Grid Technologies Conference – Latin America (ISGT Latin America)*, Gramado, Brazil, 15–18 September 2019.
- Mirjalili, S., Mirjalili, S. M. and Hatamlou, A. (2015). Multi-Verse Optimizer: A Nature-Inspired Algorithm for Global Optimization. *Neural Computing and Applications*, 27(2), pp. 495–513. doi: 10.1007/s00521-015-1870-7
- Morris, M. S. and Thorne, K. S. (1988). Wormholes in Space Time and Their Use for Interstellar Travel: A Tool for Teaching General Relativity. *American Journal on Physics*, 56, pp. 395–412. doi: 10.1119/1.15620
- Najdoska, A. and Cvetkovski, G. V. (2022). Determination of Maximum Power Point from Photovoltaic System Using Genetic Algorithm. *COMPEL – The International Journal for Computation and Mathematics in Electrical and Electronic Engineering*, 41(4), pp. 1107–1119. doi: 10.1108/COMPEL-11-2021-0445
- Najdoska, A. and Cvetkovski, G. V. (2024). Stochastic Approach for Maximum Power Point Determination for Bifacial PV Modules by Implementing Two Different Cell Models. *COMPEL - The International Journal for Computation and Mathematics in Electrical and Electronic Engineering*, 43(3), pp. 704–720. doi: 10.1108/COMPEL-11-2023-0563
- Ndegwa, R., Simiyu, J., Ayieta, E. and Odero, N. (2020). A Fast and Accurate Analytical Method for Parameter Determination of a Photovoltaic System based on Manufacturer's Data. *Journal of Renewable Energy*, 2020, pp. 1–18. doi: 10.1155/2020/7580279
- Qais, M. H., Hasanien, H. M. and Alghuwainem, S. (2022). Accurate Three-Diode Model Estimation of Photovoltaic Modules Using a Novel Circle Search Algorithm. *Ain Shams Engineering Journal*, 13(3), pp. 1–14. doi: 10.1016/j.asej.2022.101824
- Sayed, G. I., Darwish, A. and Hassanien, A. E. (2018). A New Chaotic Multi-Verse Optimization Algorithm for Solving Engineering Optimization Problems. *Journal of Experimental & Theoretical Artificial Intelligence*, 30(2), pp. 293–317. doi: 10.1080/0952813X.2018.1430858
- Steinhardt, P. J. and Turok, N. (2002). A Cyclic Model of the Universe. *Science*, 296, pp. 1436–1439. doi: 10.1126/science.1070462
- Sukhatme, S. P. (1984). *Solar Energy: Principles of Thermal Collection and Storage*. McGraw-Hill, New Delhi. Publication.
- Sun, X., Khan, M. R., Deline, C. and Alam, M. A. (2018). Optimization and Performance of Bifacial Solar Modules: A Global Perspective. *Applied Energy*, 212, pp. 1601–1610. doi: 10.1016/j.apenergy.2017.12.041
- Tegmark, M. (2004). Parallel universe. In: J. D. Barrow, P. C. W. Davies, C. L. Harper Jr., eds., *Science and Ultimate Reality: Quantum Theory, Cosmology, and Complexity*. Cambridge University Press, Cambridge, UK, pp. 459–491.
- Torres, J. P. N., Nashih, S. K. and Fernandes, C. A. F. (2018). The Effect of Shading on Photovoltaic Solar Panels. *Energy Systems*, 9, pp. 195–208. doi: 10.1007/s12667-016-0225-5
- Villalva, M. G., Gazoli, J. R. and Filho, E. R. (2009). Comprehensive Approach to Modeling and Simulation of Photovoltaic Arrays. *IEEE Transactions on Power Electronics*, 24(5), pp. 1198–1208. doi: 10.1109/TPEL.2009.2013862
- Xiao, W., Dunford, W. G. and Capel, A. (2004). A Novel Modelling Method for Photovoltaic Cells. *IEEE 35th Annual Power Electronics Specialists Conference (IEEE Cat. No.04CH37551)*, 3, pp. 1950–1956. doi: 10.1109/PESC.2004.1355416